

Magnetic edge states, spin dynamics and coherent manipulation of molecular graphene nanoribbons

Michael Slota,^{1,2} Ashok Keerthi,³ William K. Myers,² Evgeny Tretyakov,⁴ Martin Baumgarten,³ Arzhang Ardavan,^{2,5} Hatef Sadeghi,⁶ Colin J. Lambert,⁶ Akimitsu Narita,³ Klaus Müllen,³ and Lapo Bogani^{1,2}*

¹ Department of Materials, University of Oxford, 16 Parks Road, OX1 3PH, Oxford, United Kingdom.

² Centre for Advanced ESR, University of Oxford, South Parks Road, OX1 3QR, Oxford, United Kingdom.

³ Max-Planck-Institut für Polymerforschung, Ackermannweg 10, 55128, Mainz, Germany.

⁴ N. N. Vorozhtsov Novosibirsk Institute of Organic Chemistry, 9 Ac. Lavrentiev Avenue, Novosibirsk 630090, Russia.

⁵ Clarendon Laboratory, University of Oxford, Parks Road, OX1 3PU, Oxford, United Kingdom.

⁶ Quantum Technology Centre, Physics Department, Lancaster University, LA1 4YB, Lancaster, United Kingdom.

Keywords: graphene, graphene nanoribbons, molecular magnets, bottom-up synthesis.

Graphene, a single-layer network of carbon atoms, shows outstanding electrical and mechanical properties,¹ and graphene ribbons with nanometer-scale widths,^{2,3} should exhibit half-metallicity,⁴ quantum confinement and edge effects.^{5,6} Magnetic edges in graphene nanoribbons have undergone intense theoretical scrutiny, because their coherent manipulation would be a milestone for spintronic⁷ and quantum computing devices.⁸ Experimental investigations are however hampered by the fact that most nanoribbons do not have the required atomic control of the edges, and that the proposed graphene terminations are chemically unstable⁹. Here we solve both of these problems, by using molecular graphene nanoribbons functionalized with stable spin-bearing radical groups. We observe the predicted delocalized magnetic edge states, and test present theoretical models about the spin dynamics and the spin-environment interactions. Comparison with a non-graphitized reference material allows clear identification of fingerprint behaviours. We quantify the spin-orbit coupling parameters, define the interaction patterns, and unravel the spin decoherence channels. Even without any optimization, the spin coherence time is in the μs range at room temperature, and we perform quantum inversion operations between edge and radical spins. This new approach to problem of spins in well-defined electronic nanostructures offers a long-awaited experimental testbed for the theory of magnetism in graphene nanoribbons. The observed coherence times open up encouraging perspectives for the use of magnetic nanoribbons in quantum spintronic devices.

Theory predicts that graphene nanoribbons (GNRs) can have magnetic edges,⁶ which would display ferromagnetism and excellent spin filtering properties,⁷ in addition to interesting quantum-coherence

features.⁸ On the other hand, most GNRs do not have atomically-precise edges and bare graphene terminations are very sensitive to chemical modification,⁹ so that the properties of magnetic edge states, and even whether they exist at all, is still uncertain. Previous results using microscopy have largely been blind to the magnetic effects. We have developed the bottom-up molecular synthesis, allowing for the fabrication of atomically precise GNRs with various structures, which can be uniquely defined by the shape of molecular precursors.^{10,11,10} We have very recently demonstrated the synthesis of pure zigzag GNRs showing localized edge states in ultra-high vacuum, but the magnetic characterizations turned out to be highly challenging due to their instability, so that the spin properties of such well-defined zigzag GNRs remain largely unexplored.^{11,12}

We overcome these problems by injecting a spin density into the edge states of stable molecular GNRs synthesized via solution-based bottom-up chemical methods, using nitronyl-nitroxide radicals¹³ (NIT) as magnetic injectors. The advantages of this approach are that: the magnetic functionalities are well known,¹⁴ instead of relying on still-undefined magnetic states and they show interesting quantum properties;¹⁵ the sample can be mass-produced, instead of appearing just on one device; and we can test the classical and quantum spin properties in depth; the systems are chemically very stable.

The synthesis of NIT-functionalized GNRs (NIT-GNRs) starts with Diels–Alder polymerization of a bromo-functionalized tetraphenylcyclopentadienone-based monomer **1**, yielding a bromo-substituted precursor polymer **2** (Fig.1a). Palladium-catalysed cross-coupling of **2** to triphenylphosphine-gold(I)-(nitronyl nitroxide-2-ide) yields the magnetic NIT-polyphenylene, which provides a non-graphitized reference material (Fig.1b). Graphitization of **2** yields the bromo-substituted nanoribbons **3**, which are magnetically functionalized to NIT-GNRs by partial bromine substitution via cross-coupling (Fig.1c).¹⁶ Size-exclusion chromatography of **2** yields an average molecular weight of 126 kg/mol, corresponding to an average nanoribbon length $\bar{l} > 100$ nm. FTIR, Raman and UV-Vis spectroscopies corroborate the well-defined NIT-GNR structure, as in previous reports,¹⁶ without appreciable presence of transition-metal magnetic impurities (SI).

The unpaired electron of the nitronyl-nitroxide resides in a π -orbital extending over two N–O groups and a C atom, which overlaps considerably with the π -orbitals of the aromatic backbone, and is known to inject spin into aromatic substituents (SI).¹⁷ Modelling of NIT-GNRs using density functional theory shows a sizeable spin density injected into the graphene backbone, creating localized, non-dispersive states and magnetic dispersive edge state, while the spins of the NIT-polyphenylene remain in completely localized states (Fig.1b,c and SI).

We can directly observe and manipulate the spin states using electron spin resonance¹⁸ (ESR), where the spin levels are split by a magnetic field and transitions are induced by microwave absorption. Static spectra at different frequencies (Fig.2a) are reproduced using the spin Hamiltonian:

$$1) H = H_Z + H_{Hy} + H_D + H_{Ex},$$

where the Zeeman term $H_Z = \mu_B \mathbf{B} \mathbf{g} \mathbf{S}_i$ contains the effect of the magnetic field \mathbf{B} on the i -th spin \mathbf{S}_i , via the Landé tensor \mathbf{g} ; $H_{Hy} = \sum_{i,n} \mathbf{S}_i \mathbf{A}_{in} \mathbf{I}_n$ is the hyperfine interaction between the electron spin and the spin of the nucleus n ; $H_D = \sum_{i \neq j} \mathbf{S}_i \mathbf{D}_{ij} \mathbf{S}_j$ is the dipolar coupling, with $D = g_i g_j \mu_0 \mu_B^2 (4\pi \hbar r_{ij}^3)^{-1} \text{diag}(-1, -1, 2)$, that contains the vacuum permeability μ_0 , the Bohr magneton μ_B and the spin-spin distance r ; $H_{Ex} = \sum_{i \neq j} J \mathbf{S}_i \mathbf{S}_j$ represents the exchange coupling. The parameters that best reproduce all frequencies are: $\mathbf{g}=[2.0097(5), 2.0060(4), 2.0026(1)]$; hyperfine coupling with the ^{14}N atoms $\mathbf{A}_N=[0.0, 3(2), 34(2)]$ MHz, tilted by $\varphi=9^\circ$ in-plane relative to the \mathbf{g} tensor; $D_{12}=D_1=11.0 \pm 0.5$ MHz and $D_{13}=D_{23}=D_2=8.5 \pm 0.5$ MHz for the along and across-edge interactions, respectively (Fig2b). Within error, the same results are obtained for the radicals on NIT-GNRs: $\mathbf{g}=[2.0098(5), 2.0059(5), 2.0026(1)]$, $\mathbf{A}_N=[0.0, 5(2), 34(2)]$, $D_1=11.0 \pm 0.5$ MHz, $D_2=8.5 \pm 0.5$ MHz. The inter and intra-edge exchange interactions are $J_1=-25 \pm 5$ MHz, $J_2=12 \pm 3$ MHz, in agreement with the sign expected from theoretical predictions¹⁹ and Goodenough-Kanamori rules.^{13,14} These signals are to be attributed to the spin density localized on the nitronyl-nitroxides.

In addition to this signal, NIT-GNRs display the predicted edge-state as an intense feature with uniaxial anisotropy: $g_{\parallel}=2.0024(3)$, $g_{\perp}=2.0041(2)$. Metallic impurities would produce ESR linewidths of tens of mT, vs the 1-2 mT observed. Metals and spin-bearing defects in the graphene backbone would have a different hyperfine coupling than the NITs, would not display all the characteristics of NIT radicals and the DEER experiments would not be possible with randomly-placed impurities (see later).

Its shape and linewidth rule out magnetic impurities and match previous hints of delocalized spin states,²⁰ providing the smoking gun for the existence of edge spin states, long predicted for graphene nanoribbons.⁴⁻⁷ Theory predicts that the honeycomb lattice of graphene introduces an axial spin-orbit effect, Δ_{SO} , while the breaking of the mirror symmetry of the plane produces a Rashba-type transverse term, Δ_R , yielding the Hamiltonian $H_{SO} = \pm \Delta_{SO} \sigma_z S_z + \Delta_R (\pm \sigma_x S_x - \sigma_y S_y)$, where \pm denote the valley degrees of freedom, S_i and σ_i spin and pseudospin Pauli matrices.⁸ $\Delta_{SO} \approx 15$ μeV and $\Delta_R \approx 1$ μeV are extracted by considering that $|\Delta E(g_i - g_e)| = 2\Delta_i$, where g_e is the free electron value, and perturbation theory is used to account for the effect of excited states at energy ΔE (available from the *ab-initio* calculations). This constitutes a direct experimental confirmation of tight-binding estimates of spin-orbit coupling in graphene,^{21,21} and its suppression compared to carbon nanotubes, predicted by the lattice symmetry and the absence of curvature.^{5,22} These observations, together with the fact that the static spectra are largely insensitive to exchange interactions, indicate that the NIT-GNRs fall into a very interesting regime, where coherent manipulation of the spins is possible.

We thus explore the quantum spin coherence using time-resolved ESR. The quantum evolution of a spin can be represented as a movement over the Bloch sphere, with zenithal positions pure $|1/2\rangle$ and $|-1/2\rangle$ states, and all their possible combinations mapped on the sphere (Fig.3a). The spin-relaxation-time, T_1 , represents spin-flips (vertical displacement), while the phase-memory-time, T_2 , describes the evolution of

the quantum phase information (azimuthal movement). We measure T_I via the picket-fence technique²³ and T_m (a measure of the dephasing time) by the Hahn-echo decay. We fit the echo-signal Y with an exponential function $Y(\tau) = Y_0 e^{-\left(\frac{2\tau}{T_m}\right)^x} [1 + k_1 \sin(2\omega\tau + \varphi_1) + k_2 \sin(4\omega\tau + \varphi_2)] + c$ that contains modulation by the environment at a frequency ω (amplitudes k_1 and k_2 for first- and second-order effects) and a stretch parameter x (Fig.3b). We always find $x=1$, indicating that the relaxation time approximation is good, successive events are uncorrelated, and $T_m \approx T_2$ as traditionally defined.²⁴

The T_1 values, $\sim 10^{-5}$ s, validate theoretical predictions by analytical methods.²⁵ The temperature-dependence of T_1^{-1} (Fig.3c) shows three main regimes: a linear one below 25 K, characteristic of spin-phonon energy transfers; a Raman region between 25 and 200 K, where relaxation happens via virtual states; a room-temperature region where local vibrational modes play a role, with the same characteristic energy (1354 cm^{-1}) for NIT-GNR and NIT-polyphenylene, tentatively assigned to the N–O stretching mode. Theories of low-temperature spin-phonon relaxation in graphene^{5,21} quantum dots consider a deformation-potential-mechanism, active for longitudinal-acoustic phonons, and a bond-length-change mechanism, active for transversal- and longitudinal-acoustic modes. These, in conjunction with the absence of Van Vleck cancellation,²¹ are predicted to generate the linear dependence indeed observed here, at low fields. The other hypothesized mechanism, spin-state-admixture,⁵ can be ruled out by the observed temperature- and field-dependences and the low value of the observed Rashba spin-orbit-coupling, to which it is linked by symmetry selection rules.^{5,21}

Even without any optimization, NIT-GNRs display $T_m=0.5 \mu\text{s}$ at room-temperature and $1.1 \mu\text{s}$ at 85 K (Fig.3c and SI), 100 times longer than the 12 ns available in spintronic devices.²⁶ The high value is likely linked to the efficient suppression of scattering in atomically-regular edges. NIT-GNRs show only a slight increase of T_m at lower temperatures, while NIT-polyphenylene shows a minimum at 170 K and a broad maximum at 60 K, attributable to the progressive freezing of the benzene-benzene σ -bonds in the backbone. Although T_m for the localized radicals in NIT-polyphenylene might be slightly longer, the NIT-GNRs allow validating theories of spin relaxation in graphene, possess an edge-state that is connected to transport and is promising for quantum operations.

We now proceed to determine the sources of decoherence in NIT-GNRs. The modulation of the Hahn-echo amplitude (Fig.3b) at $\omega/2\pi=3.6 \text{ MHz}$, a frequency typical of ^{13}C spin-nuclei interactions, suggests that hyperfine decoherence channels are important. Electron-electron-double-resonance-detected-nuclear-magnetic-resonance, EDNMR, allows de-convoluting the different nuclear contributions^{17,23} (Fig.4a). ^{14}N coupling is dominant, confirming the analysis of CW spectra, but ^{13}C , ^1H single-quantum-transitions, ^{14}N , ^{13}C double-quantum-transitions and nitrogen-carbon mixed-transitions also play an important role. The coupling strength to the ^{13}C of the graphene backbone $\sim 10\text{MHz}$, is considerably smaller than theoretical estimates for confined graphene dots,^{5,27} where anisotropic, Fermi-contact and nucleus-orbital interactions

contribute to a total ^{13}C hyperfine interaction of ~ 70 MHz. These couplings suggests that nuclei could be used as computational resources.²⁸

We eventually consider the coupling between localized spins and the edge state. Information about electron-electron interactions is obtained by four-pulse double-electron-electron-resonance (DEER, Fig.4b),²⁹ where the system is initialised and probed at the g_x resonance of the radicals, and perturbed at the resonance condition of the edge-state. The resulting spectrum displays an intriguing slow oscillation that is overlaid with fast ones (Fig.4c). The fast period corresponds to the D_1 and D_2 interactions, which are too strong for accurate resolution using DEER, and are better appreciated via the CW spectra. Slow oscillations correspond to interactions between localized and edge-state spin yielding a radical-edge spin interaction of 3 MHz (Fig.4d); these oscillations are absent in NIT-polyphenylene, in agreement with the lack of edge-states. The extracted edge-radical spin-inversion time, ~ 330 ns, is considerably shorter than T_m , enabling coherent inversion operations using graphene edge-states and localized spins. This, in conjunction with recent results on the transport on molecular nanoribbons, opens fascinating possibilities: quantum operations can in principle be performed via single-electron transport,³⁰ and the spin states detected electrically,³¹ so that our radical-substituted NIT-GNRs seem ideal candidates for quantum nanoelectronic devices. The interaction of multiple radical spins with a coherent, delocalized edge-state, could allow a single flowing electron to transmit entanglement along the spin ensemble.^{8,32} Furthermore, such molecular nanoribbons are a useful testbed for fundamental theories of graphene, and our measurements of spin-orbit, hyperfine and edge-spin coupling already disclose a physics that would otherwise be accessible only by overcoming present challenges in quantum-Hall-effect studies at sub-mK temperatures.^{21,22} Detailed access to the spin dynamics, together with an atomically-defined structure, opens the path to the quantitative analysis of spin-phonon interactions in graphene dots. The study of different molecular spin-injectors and of different aromatic backbones,¹⁰ e.g. to modulate the spin coupling, opens up a new area of chemistry that mixes molecular magnetism and graphene. Environmental effects, such as GNR-GNR or GNR-substrate interactions are an interesting future area of research and calculations show, encouragingly, no detrimental effect on the spin density by deposition on h-BN (SI). With respect to applications, since a dominant decoherence channel is ^{14}N hyperfine coupling, there is ample room to increase T_2 , e.g. by, dynamic nuclear spin polarization³³, isotopic substitution³⁴ or chemical engineering³⁵. Full investigations of magnetic doping effects and of incomplete edge functionalization with radicals is currently underway, and will introduce graphene nanoribbons as a powerful tool to investigate finite-size-effects in quantum Heisenberg spin-chains.¹⁹

Acknowledgments

We thank the European Research Council (ERC-StG 338258 OptoQMol), the EU (COST-CA15128, MOLESCO-606728 and Graphene Flagship), EPSRC (QuEEN grant), the Royal Society (University

Research Fellowship and URF grant), RFBR (17-53-50043), the Max Planck Society and German DAAD Bilateral Exchange of Academics (2015/50015739) for financial support.

Author contributions

M.S. and W.M. performed the ESR characterization. A.K. and E.T. performed the synthesis and related characterization, for which M.B., A.N and K.M. provided supervision. H.S. and C.J.L. performed the numerical modelling. M.S., W.M, A.A. and L.B. contributed to the ESR data analysis. M.S., A.N., K.M. and L.B. conceived the experiments and M.S. and L.B. wrote the manuscript. All authors contributed to the discussion and to the final version of the manuscript.

Additional information

The authors declare no competing financial interests. Supplementary information accompanies this paper.

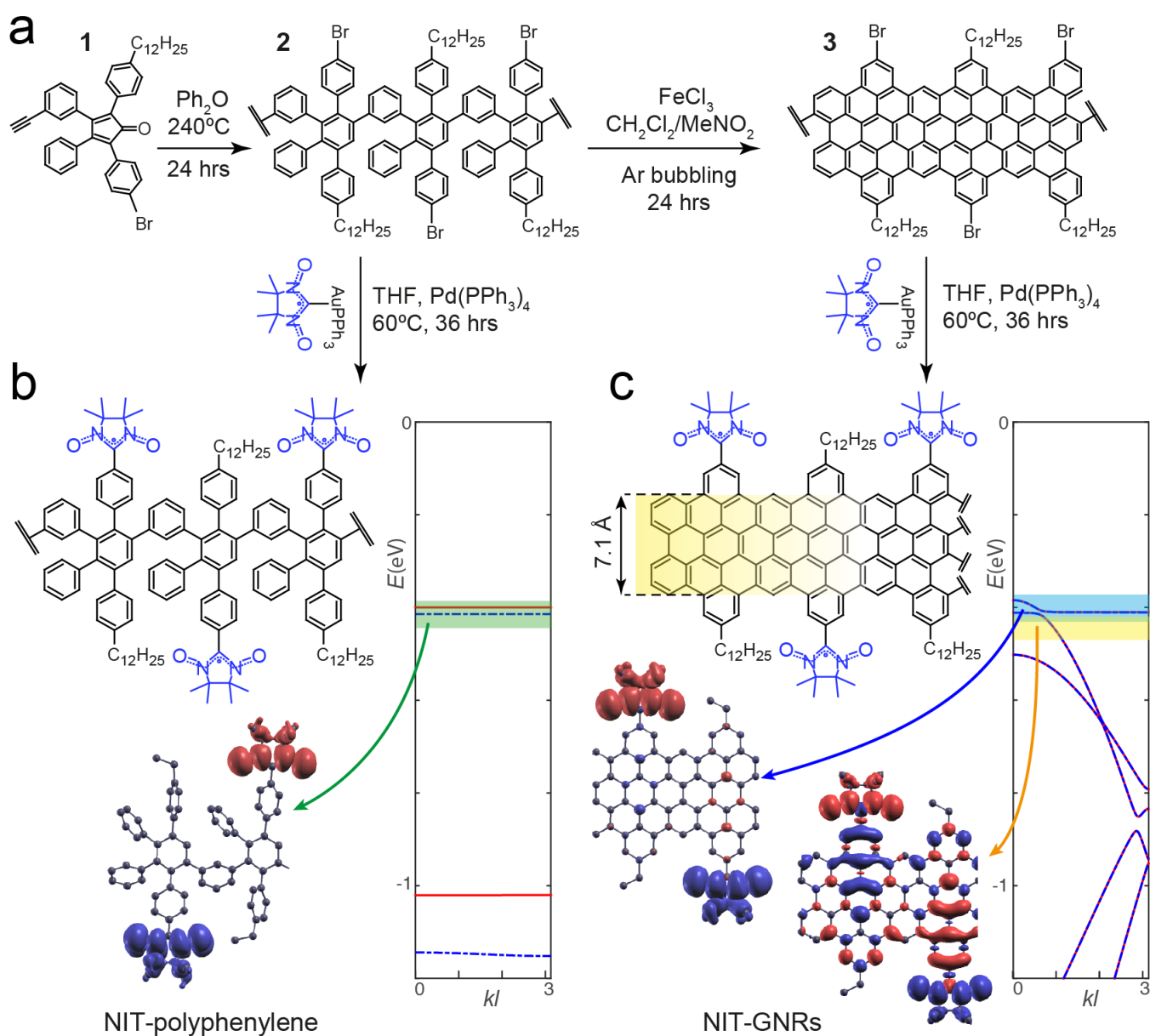


Figure 1. Functionalized graphene nanoribbons: a) Synthetic route used to create both the non-graphitized NIT-polyphenylene and NIT-GNRs (nitronyl-nitroxide spin-bearing radicals highlighted in blue). b) NIT-polyphenylene schematic structure (top), and calculated local density of states for spin up and down (bottom). The spin-resolved energy level diagram (plotted against the wavevector k times the repeating unit length l) shows no band structure and a localized density on the NIT groups (green arrow). c) Structurally well-defined NIT-GNRs, showing the graphene nanoribbon backbone functionalized with radicals (top). The resulting spin-resolved band structure (right), shows localized states and spin injection inside delocalized edge states. Densities calculated for different energy ranges are depicted (azure and orange shaded areas and arrows), with blue and red referring to local densities of spin up and down states, for a given energy interval.

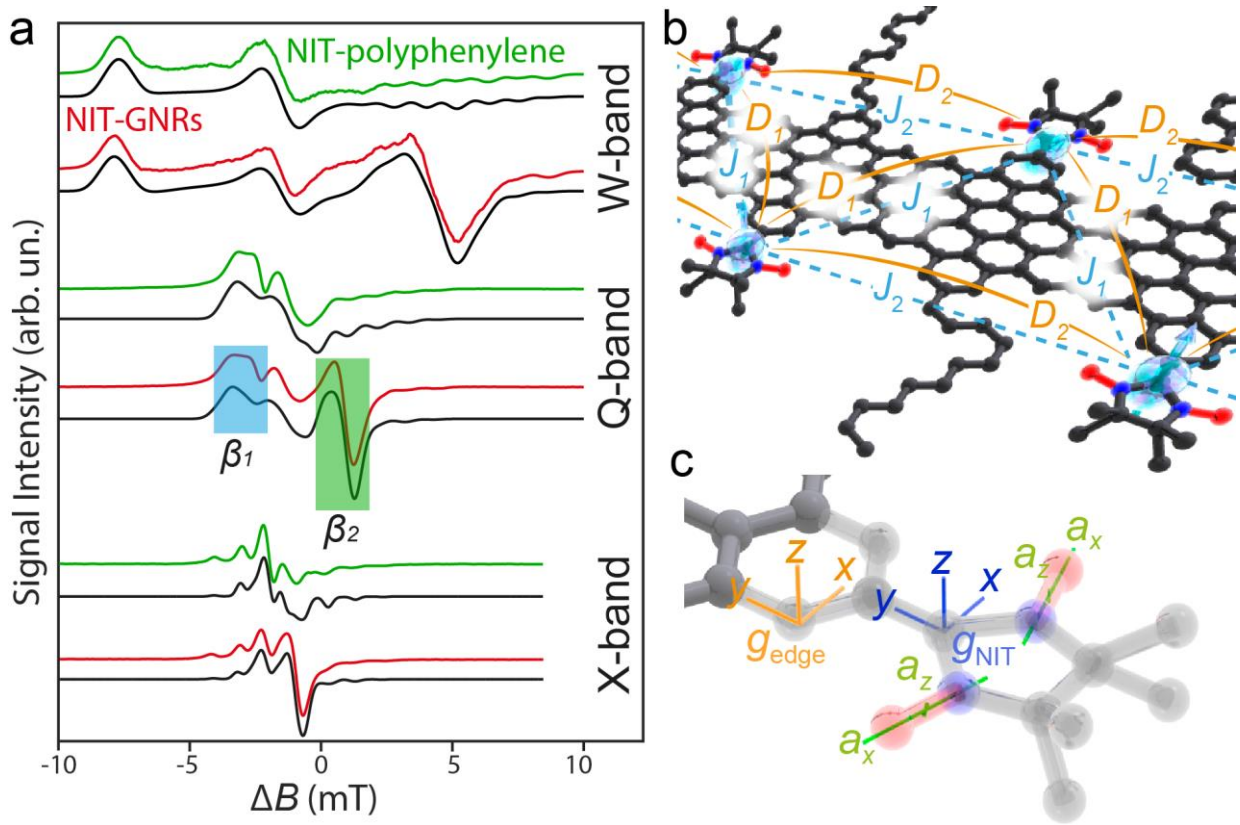


Figure 2. Static spectra and magnetic interaction pathways. a) ESR spectra for NIT-polyphenylene (green) and NIT-GNRs (red), at three frequencies. Spectra are plotted against the magnetic field from the edge state resonance, ΔB . Black lines are simulations to the spectra. DEER pump and probe windows for Fig.4 are β_1 and β_2 , respectively. b) Spin interaction pathways for the localized spin density of the radical groups, showing the J_1 and J_2 exchange interactions (blue) and the dipolar interactions D_1 and D_2 (orange). c) Orientation of the ^{14}N hyperfine interaction channel (green), with the lengths of the axes proportional to the principal tensor elements (a_y is smaller than the axis width). The orientation of the local g tensor frame of the radical (blue) and that of the graphene edge state (orange) are also depicted.

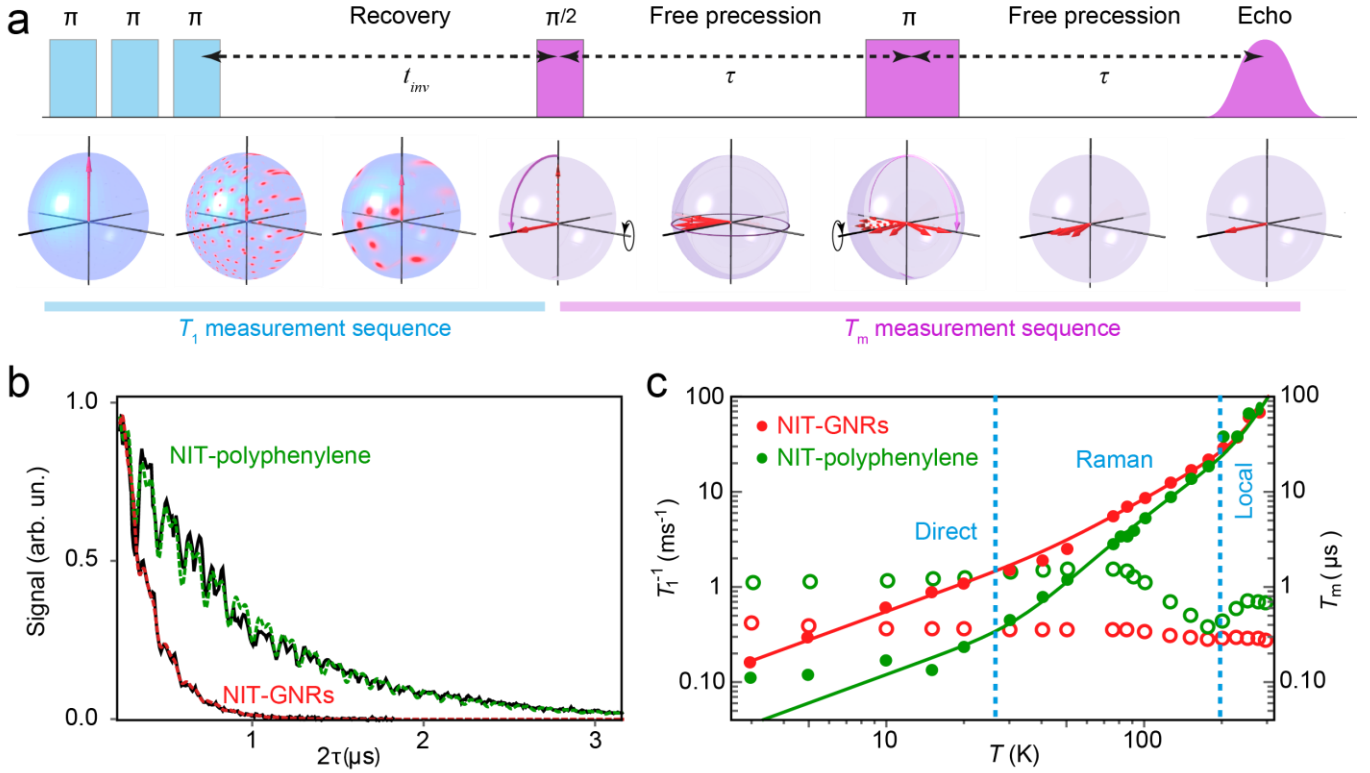


Figure 3. Spin-lattice and coherence times. a) Pulse sequence used to extract the spin relaxation times, and effect the Bloch-sphere in the rotating-wave frame. Using a picket-fence series of π -pulses (blue boxes) the spin polarization (red arrow) is abolished and let recover after a time T_1 . The spins are then rotated to the xy-plane with a $\pi/2$ -pulse (violet box) and let free to precess around the z-axis at an undetermined rate, for a time τ . A π -rotation around the y-axis in the middle of the free precession causes an echo signal when the spins regroup (red bell). b) X-band Hahn-echo signal vs delay time τ for NIT-GNRs and NIT-polyphenylene, at 85 K. Red and green lines are fits to the data, yielding T_m . c) T_1^{-1} (full dots, left axis) and T_m (open dots, right axis) vs temperature for NIT-GNRs (red) and NIT-polyphenylene (green), at 9.4 GHz. Lines are simulations for T_1^{-1} (see text), the dashed lines separate the different regimes of spin-lattice relaxation.

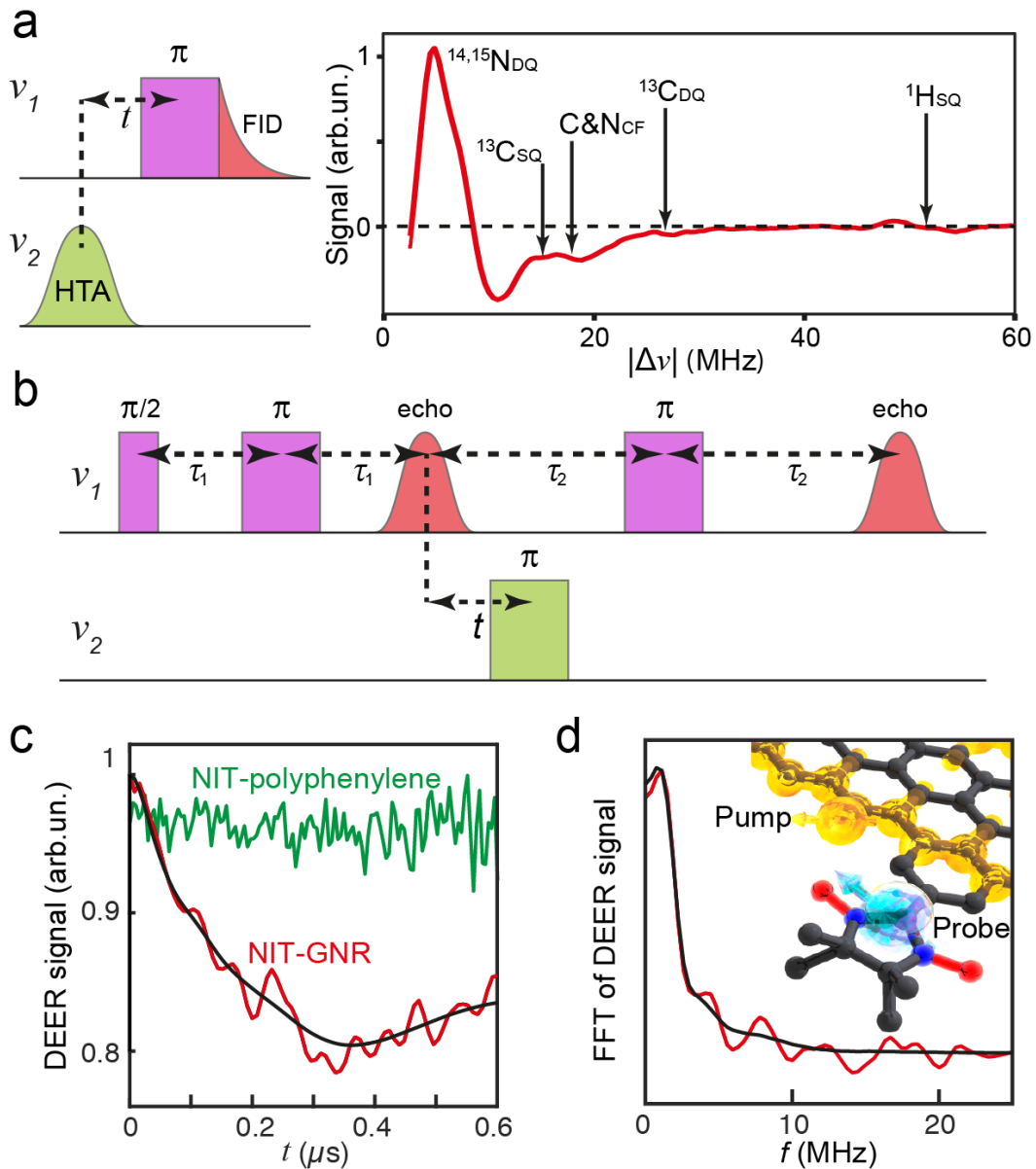


Figure 4. Hyperfine coupling and multi-spin operability in nanoribbons. a) Double electron-electron detected nuclear magnetic resonance (EDNMR) of the NIT-GNRs, with the pulse sequence used on the left and the resulting spectrum and assignment on the right, as obtained at Q-band at 85 K, showing the single-quantum (SQ), double-quantum (DQ) and combination-frequency (CF) transitions of the different nuclei coupled to the electron. The high-turning-angle (HTA) pulse is set at ν_2 , i.e. the edge-state-resonance β_2 (Fig.2a), while ν_1 is swept. b) Sequence used to determine the spin-spin interactions and perform edge-local spin quantum inversion operations via double electron-electron resonance (DEER), with ν_1 set at the localized spin resonance and ν_2 at the edge state (β_1 and β_2 in Fig.2a). c) Background-corrected time-domain DEER spectrum for NIT-polyphenylene (green) and NIT-GNRs (red). The black line singles out the low-frequency interactions. d) Fast Fourier transform (FFT) of the DEER signal of NIT-GNRs, showing the interaction energy spectrum characteristic of two-spin operations. The black line singles out the contribution from edges interacting with localized spins, pictorially depicted in the drawing.

Bibliography:

- ¹ Castro Neto, A. H., Guinea, F., Peres, N. M. R., Novoselov, K. S. & Geim, A. K. The electronic properties of graphene. *Rev. Mod. Phys.* **81**, 109 (2009).
- ² Jiao, L., Zhang, L., Wang, X., Diankov, G., & Dai, H. Narrow graphene nanoribbons from carbon nanotubes. *Nature* **458**, 877-880 (2009).
- ³ Jia, X., Hofmann, M., Meunier, V., Sumpter, B.G., Campos-Delgado, J., Romo-Herrera, J.M., Son, H., Hsieh, Y.P., Reina, A., Kong, J. and Terrones, M. Controlled formation of sharp zigzag and armchair edges in graphitic nanoribbons. *Science*, **323**, 701-1705 (2009).
- ⁴ Son, Y. W., Cohen, M. L., & Louie, S. G. Half-metallic graphene nanoribbons. *Nature* **444**, 347-349 (2006).
- ⁵ See, for a review: Recher, P., & Trauzettel, B. Quantum dots and spin qubits in graphene. *Nanotechnology*, **21**, 302001(2010). And references therein.
- ⁶ Meunier, V., Souza Filho, A. G., Barros, E. B., & Dresselhaus, M. S. Physical properties of low-dimensional sp_2 -based carbon nanostructures. *Review of Modern Physics* **88**, 025005 (2016).
- ⁷ Pesin, D., & MacDonald, A. H. Spintronics and pseudospintronics in graphene and topological insulators. *Nature Materials* **11**, 409-416 (2012).
- ⁸ Trauzettel, B., Bulaev, D. V., Loss, D., & Burkard, G. Spin qubits in graphene quantum dots. *Nature Physics* **3**, 192-196 (2007)
- ⁹ Kunstmann, J., Özdoğan, C., Quandt, A., & Fehske, H. Stability of edge states and edge magnetism in graphene nanoribbons. *Physical Review B*, **83**, 045414 (2011). Barone, V., Hod, O., & Scuseria, G. E. Electronic structure and stability of semiconducting graphene nanoribbons. *Nano letters* **6**, 2748-2754 (2006).
- ¹⁰ Narita, A., Wang, X.-Y., Feng, X. & Müllen, K. New advances in nanographene chemistry *Chem. Soc. Rev.* **44**, 6616-6643 (2015).
- ¹¹ Ruffieux, P., Wang, S., Yang, B., Sánchez-Sánchez, C., Liu, J., Dienel, T., Talirz, L., Shinde, P., Pignedoli, C. A., Passerone, D., Dumslaff, T., Feng, X., Müllen, K., & Fasel, R. On-surface synthesis of graphene nanoribbons with zigzag edge topology. *Nature* **531**, 489-492 (2016).
- ¹² Cai, J., Ruffieux, P., Jaafar, R., Bieri, M., Braun, T., Blankenburg, S., Muoth, M., Seitsonen, A.P., Saleh, M., Feng, X. & Müllen, K. Atomically precise bottom-up fabrication of graphene nanoribbons. *Nature* **466**, 470-473 (2010).
- ¹³ Luneau, D., & Rey, P. Magnetism of metal-nitroxide compounds involving bis-chelating imidazole and benzimidazole substituted nitronyl nitroxide free radicals. *Coordination chemistry reviews* **249**, 2591-2611 (2005).

-
- ¹⁴ Caneschi, A., Gatteschi, D. & Rey, P. The Chemistry and Magnetic Properties of Metal Nitronyl Nitroxide Complexes. *Progress in Inorganic Chemistry* **39**, 331 (1991).
- ¹⁵ Collauto, A., Mannini, M., Sorace, L., Barbon, A., Brustolon, M., & Gatteschi, D. A slow relaxing species for molecular spin devices: EPR characterization of static and dynamic magnetic properties of a nitronyl nitroxide radical. *Journal of Materials Chemistry* **22**, 22272-22281 (2012).
- ¹⁶ Narita, A., Feng, X., Hernandez, Y., Jensen, S.A., Bonn, M., Yang, H., Verzhbitskiy, I.A., Casiraghi, C., Hansen, M.R., Koch, A.H., Fytas, G., Ivasenko, O., Li, B., Mali, K.S., Balandina, T., Mahesh, S., De Feyter, S. & Müllen, K. Synthesis of structurally well-defined and liquid-phase-processable graphene nanoribbons. *Nature Chemistry* **6**, 126-132 (2014).
- ¹⁷ Zheludev, A., Barone, V., Bonnet, M., Delley, B., Grand, A., Ressouche, E., Rey, P., Subra, R. & Schweizer, J. Spin-density in a nitronyl nitroxide free-radical-polarized neutron-diffraction investigation and ab-initio calculations. *Journal of the American Chemical Society*, **116**, 2019 (1994).
- ¹⁸ Schweiger, A., & Jeschke, G. *Principles of pulse electron paramagnetic resonance*. Oxford University Press, Oxford, UK (2001).
- ¹⁹ Golor, M., Wessel, S., & Schmidt, M. J. Quantum nature of edge magnetism in graphene. *Physical review letters* **112**, 046601 (2014).
- ²⁰ Rao, S.S., Stesmans, A., van Tol, J., Kosynkin, D.V., Higginbotham-Duque, A., Lu, W., Sinitskii, A. & Tour, J.M. Spin dynamics and relaxation in graphene nanoribbons: electron spin resonance probing. *ACS nano* **6**, 7615-7623 (2012).
- ²¹ Min, H., Hill, J. E., Sinitsyn, N. A., Sahu, B. R., Kleinman, L., & MacDonald, A. H. Intrinsic and Rashba spin-orbit interactions in graphene sheets. *Physical Review B* **74**, 165310 (2006).
- ²² Kane, C. L. & Mele, E. J. Z_2 Topological Order and the Quantum Spin Hall Effect. *Physical Review Letters* **95**, 146802 (2005).
- ²³ Eaton, G. R. & Eaton, S. S. Multifrequency Electron Spin-Relaxation Times. *Multifrequency Electron Paramagnetic Resonance: Theory and Applications* (Ed. Misra, S. K., Wiley-VCH Verlag GmbH & Co. KGaA, Weinheim, Germany, 2011).
- ²⁴ Klauder, J. R. & Anderson, P. W. Spectral diffusion decay in spin resonance experiments. *Physical Review* **125**, 912 (1962).
- ²⁵ Struck, P. R. & Burkard, G. Effective time-reversal symmetry breaking in the spin relaxation in a graphene quantum dot. *Phys. Rev. B* **82**, 125401 (2010).
- ²⁶ Drögeler, M., Franzen, C., Volmer, F., Pohlmann, T., Banszerus, L., Wolter, M., Watanabe, K., Taniguchi, T., Stampfer, C. & Beschoten, B. Spin lifetimes exceeding 12 ns in graphene nonlocal spin valve devices. *Nano Letters* **16**, 3533 (2016).
- ²⁷ Fisher, J., Trauzettel, B. & Loss, D. Hyperfine interaction and electron-spin decoherence in graphene and carbon nanotube quantum dots. *Physical Review B* **80**, 155401 (2009).

-
- ²⁸ Dutt, M.G., Childress, L., Jiang, L., Togan, E., Maze, J., Jelezko, F., Zibrov, A.S., Hemmer, P.R. & Lukin, M.D., Quantum register based on individual electronic and nuclear spin qubits in diamond. *Science* **316**, 1312-1316 (2007).
- ²⁹ Ardavan, A., Bowen, A.M., Fernandez, A., Fielding, A.J., Kaminski, D., Moro, F., Muryn, C.A., Wise, M.D., Ruggi, A., McInnes, E.J. & Severin, K. Engineering coherent interactions in molecular nanomagnet dimers. *Quantum Information* **1**, 15012 (2015).
- ³⁰ Hanson, R., Kouwenhoven, L. P., Petta, J. R., Tarucha, S., & Vandersypen, L. M. Spins in few-electron quantum dots. *Reviews of Modern Physics* **79**, 1217 (2007).
- ³¹ Petta, J.R., Johnson, A.C., Taylor, J.M., Laird, E.A., Yacoby, A., Lukin, M.D., Marcus, C.M., Hanson, M.P. & Gossard, A.C. Coherent manipulation of coupled electron spins in semiconductor quantum dots. *Science* **309**, 2180 (2005).
- ³² Rycerz, A., Tworzydło, J., & Beenakker, C. W. J. Valley filter and valley valve in graphene. *Nature Physics*, **3**, 172-175 (2007).
- ³³ Foletti, S., Bluhm, H., Mahalu, D., Umansky, V. & Yacoby, A. Universal quantum control of two-electron spin quantum bits using dynamic nuclear polarization. *Nature Physics* **5**, 903-908 (2009).
- ³⁴ Balasubramanian, G., Neumann, P., Twitchen, D., Markham, M., Kolesov, R., Mizuochi, N., Isoya, J., Achard, J., Beck, J., Tissler, J., Jacques, V., Hemmer, P.R., Jelezko, F. & Wrachtrup, J. Ultralong spin coherence time in isotopically engineered diamond. *Nature Materials* **8**, 383-387 (2009).
- ³⁵ Shiddiq, M., Komijani, D., Duan, Y., Gaita-Ariño, A., Coronado, E. and Hill, S. Enhancing coherence in molecular spin qubits via atomic clock transitions. *Nature* **531**, 348-351(2016).